

# Silicon arrays as four-port optical splitting controller for terahertz band

XIAOQING ZHU, BO WANG\*, YUSEN HUANG, ZHICHAO XIONG, JIAHAO LI, XIAOFENG WANG, HONG ZOU, JINHAI HUANG, WEIYI YU

*School of Physics and Optoelectronic Engineering, Guangdong University of Technology, Guangzhou 510006, China*

A four-port terahertz beam splitter with a metallic aluminum reflecting layer is proposed, which offers high efficiency, effective zeroth-order suppression and polarization-independent properties. The grating parameters are optimized by means of rigorous coupled-wave analysis and simulated annealing. The optimized grating has a diffraction efficiency of 24.72% and 23.82% for  $\pm 1$ st and  $\pm 2$ nd orders respectively under transverse electric polarization, and 24.64% and 24.12% for  $\pm 1$ st and  $\pm 2$ nd orders respectively under transverse magnetic polarization at 118.83  $\mu\text{m}$  polarization (i.e. 2.52 terahertz band). In addition, the electric field distribution map of the beam splitter can be analyzed by the finite element method, which can well explain the optical transmission mechanism inside the grating. The simple structure of the target grating and the good process tolerance also take advantage in its practical application.

(Received December 25, 2021; accepted October 5, 2022)

*Keywords:* Terahertz device, Grating beam splitter, Polarization independent

## 1. Introduction

Terahertz (THz) waves [1, 2] are electromagnetic waves with frequencies in the range of 0.1 to 10 THz, between the microwave and infrared. THz waves are the last band in the electromagnetic spectrum that has not been fully exploited and utilized. Due to the special nature of its spectrum, THz has excellent characteristics that other spectrums do not possess, which making it an important academic and application value. For example, the terahertz band has good transparency for cloth and plastic products, excellent reflective properties for metallic materials, and minimal damage to human health. Refs. [3, 4] described a few optical devices for terahertz-based imaging at 2.52 THz, which was the radiation frequency of the far infrared CO<sub>2</sub> laser [4]. Ref. [3] carried out a SIFIR-50 from Coherent, Inc. as the THz source. Pumping by a CO<sub>2</sub> laser, it can generate cw THz output and operate stably at 2.52 THz. Grating-based terahertz imaging systems have also been widely proposed in recent years [5]. For example, in Ref. [5] the authors proposed a terahertz imaging system for terahertz referenceless wavefront sensing by computational shear interferometry, where a grating-based beam splitter structure plays an important role in the overall system. Beam splitter [6-9] is an important device in optical systems that separates the optical signal into two mutually orthogonal polarized light and transmits it along different paths. It is widely used in fiber optic communication [10, 11], optical computing [12, 13], optical storage [14, 15], biology optics [16], image processing [17] and precision measurement [18-22]. Among them, the equal-intensity

even-type beam splitter that eliminates zeroth-order diffraction spectral points has attracted widespread interest due to its unique applications in the fabrication of linear chirp phase masks for fiber-optic gratings, beam splitting for lithography optical systems [23-25], denoising for digital holographic optical systems and other applications with high zeroth-order diffraction elimination requirements.

Recently, Huang et al. successfully designed a multifunctional terahertz beam splitter in which the diffraction efficiency of each diffraction order exceeded 23.5% for both transverse electric (TE) and transverse magnetic (TM) polarizations in a four-port beam splitter [26]. In addition, Huang et al. proposed a terahertz even beam splitter in which a diffraction efficiency of more than 23% was obtained for each diffraction order under normal incidence for TE-polarized light [27]. The diffraction efficiencies of all the above papers are not satisfactory and the process tolerances [28] need to be further improved. Therefore, it is a challenging practical problem to achieve high diffraction efficiency and high homogeneity in the elimination of the zeroth-order diffraction even beam splitting in a binary simple periodic structure.

In this paper, a four-port reflective beam splitter with polarized light incident normally and a metal aluminum reflective layer at 2.52 THz terahertz band is designed by applying the rigorous coupled-wave analysis (RCWA) [29-31] as well as the simulated annealing (SA) method [32, 33] to achieve high diffraction efficiency, high uniformity and effective suppression of zeroth-order even splitting, breaking through the limitations of the traditional scalar method design, and finite element analysis (FEM) [34-37]

was used to analyze the beam splitter electric field distribution to understand the light transmission mechanism inside the grating. In addition, a tolerance analysis of the grating is carried out to obtain the allowable deviation range of the beam splitter mechanism parameters (including the thickness of grating ridge, grating period, duty cycle and incident wavelength), which is a guideline for device design and fabrication.

## 2. Grating structure and parameter optimization

A schematic diagram of a terahertz four-port reflective beam splitter is shown in Fig. 1, which consists of a single grating ridge layer and a reflective layer. The ridge layer consists of Si (refractive index  $n_1=3.42$ ) with a thickness of  $h_1$  and a width of  $w$ . The reflective layer consists of Al (refractive index  $n_2=304.71-i*376.74$  [38]) with a thickness of  $h_2$ , and  $h_2$  is set to be  $0.10 \mu\text{m}$  for the target grating structure discussed in this paper and is not involved in the optimization. In further, a plane wave (with a wavelength of  $\lambda=118.83 \mu\text{m}$ , i.e., a frequency of  $2.52 \text{ THz}$ ) is incident into the grating from an air medium with a refractive index of  $n_0=1.00$ , meanwhile  $d$  for grating period and  $f$  for duty cycle (defined as  $f=w/d$ ). Under normal incidence conditions, the target grating can split the TE and TM incident light into four beams when the period  $d$  is between  $2\lambda$  and  $3\lambda$ .

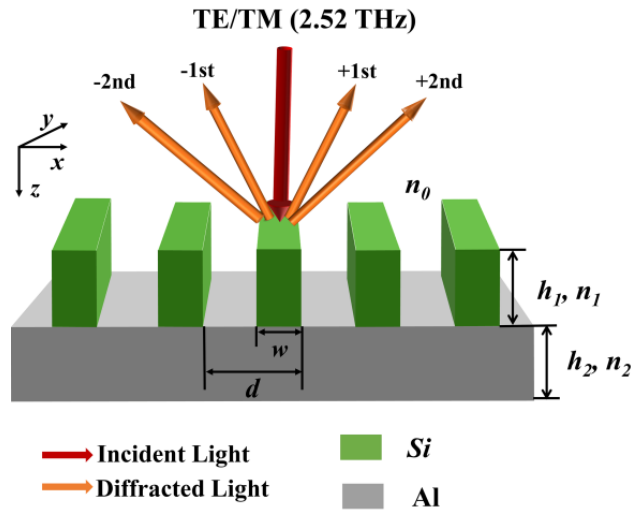


Fig. 1. Schematic of a four-port reflective grating under normal incidence (color online)

In this paper, in order to better calculate the diffraction

efficiency in both polarization states, the theoretical modelling process uses the RCWA to complete the calculation of the diffraction efficiency of the target grating and to more rapidly screen and optimize the grating parameters from the massive data. In this paper, a grating period is chosen as the target, periodic boundary conditions are set in the  $x$ -axis direction, and the diffraction efficiency of each diffraction order is obtained by coupling the boundary conditions in the grating region.

Further, this paper also applies the SA, which combines probabilistic jumps to find the global optimal solution of the objective function randomly in the solution space. Due to the normal incidence, the diffraction efficiency is the same at  $\pm 1$ st orders as well as  $\pm 2$ nd orders respectively, and the optimization parameters include  $\{d, f, h_1\}$ , and the objective function of the SA method is [32, 33]:

$$\phi(h_1, d, f) = [1 - (DE_{total} - |DE_{-1} - DE_{-2}|)], \quad (1)$$

where  $DE_{total}$  represents the sum of the diffraction efficiencies of the non-zero diffraction orders at each polarization.  $DE_{-1}$  and  $DE_{-2}$  represent the diffraction efficiency at -1st and -2nd orders under TE or TM polarization respectively. However, Eq. (1) can only calculate the optimal parameters for a single polarization. In order to obtain a polarization independent beam splitter, the cost function needs to be rewritten as:

$$\phi = \frac{\phi_{TE} + \phi_{TM}}{2}, \quad (2)$$

where  $\phi_{TE}$  and  $\phi_{TM}$  are the cost function for TE polarization and TM polarization, respectively. The optimized grating structure parameters are:  $d=257.10 \mu\text{m}$ ,  $h_1=213.20 \mu\text{m}$  and  $f=0.349$ . The optimized grating has a diffraction efficiency of 24.72% and 23.82% for  $\pm 1$ st and  $\pm 2$ nd orders respectively, under TE polarization, and 24.64% and 24.12% for  $\pm 1$ st and  $\pm 2$ nd orders, respectively, under TM polarization at a wavelength of  $118.83 \mu\text{m}$  at normal incidence. The comparison of efficiencies between this work and reported structures is given in Table 1.

Table 1. Comparison of efficiencies between this work and reported Refs. [26, 27]

Scheme	$\eta_{\pm 1}^{\text{TE}}$ (%)	$\eta_{\pm 2}^{\text{TE}}$ (%)	$\eta_{\pm 1}^{\text{TM}}$ (%)	$\eta_{\pm 2}^{\text{TM}}$ (%)
Ref. [26]	24.22%	23.89%	24.05%	23.70%
Ref. [27]	23.06%	23.06%	/	/
This work	24.72%	23.82%	24.64%	24.12%

Noteworthy, an even beam splitter with good beam splitting performance requires the uniformity of the diffraction efficiencies of each non-zeroth diffraction order in addition to the de-zeroing of the diffraction orders and the maximization of the sum of the efficiencies of the diffraction orders. The uniformity of the efficiency of each diffraction order of a beam splitter is expressed in terms of  $U$ , as:

$$U = \frac{(\eta_{\max} - \eta_{\min})}{(\eta_{\max} + \eta_{\min})}, \quad (3)$$

where  $\eta_{\max}$  and  $\eta_{\min}$  are the maximum and minimum diffraction efficiencies of the non-zeroth diffraction orders of the even beam splitter, respectively.

In order to better understand the physical process of light transmission inside the grating and to check the results of the RCWA, the FEM is used to calculate the optimized grating electric field distribution. Fig. 2 shows the normalized electric field distribution of the terahertz grating beam splitter at two polarizations. It is clear from Fig. 2 that the energy distribution from the grating ridge to the reflector layer at a normal incidence of 118.83  $\mu\text{m}$  incident light. Figs. 2 (a, b) depict the beam splitting effect of the target grating under TE and TM polarizations respectively. Due to the periodic structure of the grating, the energy distribution inside the grating shows a periodic characteristic. At the same time, the light has the property of propagating parallel to the  $x$ -axis due to the normal incidence of the incident light. Fig. 2 (a) shows the electric field distribution of light propagation under TE polarization, which shows that the energy is mainly concentrated inside the grating ridges, and for each grating ridge there is a certain symmetrical area distribution characteristic. Meanwhile, Fig. 2 (b) shows the electric field distribution of light propagation under TM polarization, where the energy is concentrated in the grating grooves near the grating ridges, which also has a symmetrical regional distribution.

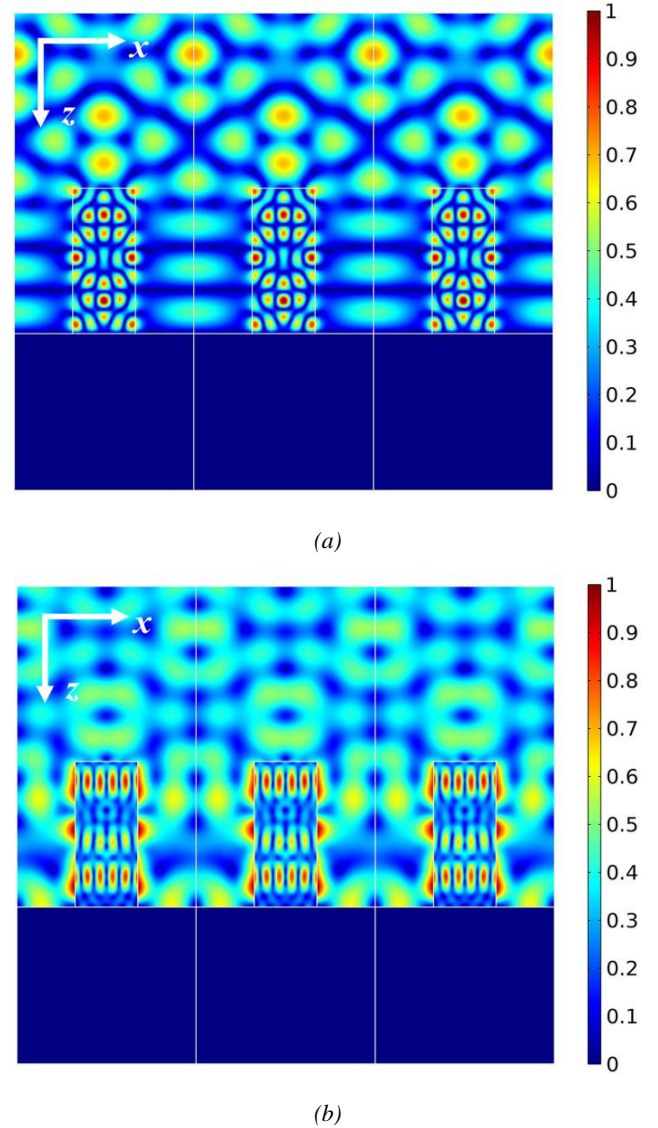


Fig. 2. Normalized electric field distribution diagram of the encapsulated grating under normal incidence: (a) TE polarization (b) TM polarization (color online)

### 3. Discussion and analysis

#### 3.1. Angular and wavelength characteristics analysis

Fig. 3 shows a plot of the incident light wavelength versus diffraction efficiency under the condition of normal incidence of the incident light. It can be seen that when the wavelength  $\lambda$  is in the range 118.707-118.924  $\mu\text{m}$ , the diffraction efficiency of each diffraction for the both polarizations order exceeds 21%. It indicates that the target grating has a good wavelength bandwidth and maintains good diffraction performance over a wide range of wavelengths, which is of great importance for its practical application.

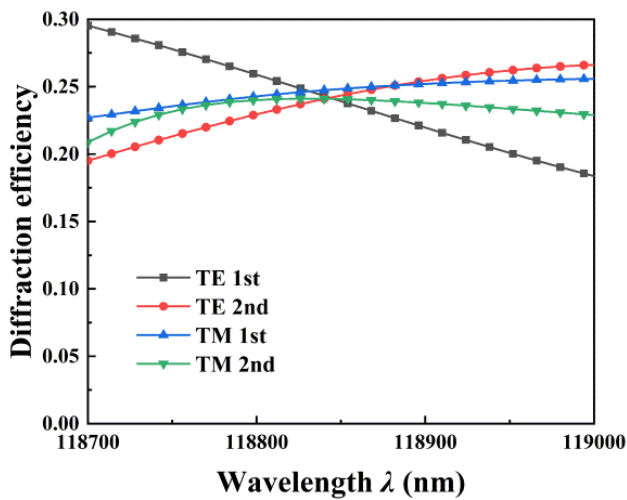


Fig. 3. The relationship between efficiency and incident wavelength for both two polarizations under normal incidence with  $d=257.10 \mu\text{m}$ ,  $f=0.349$ , and  $h_1=213.20 \mu\text{m}$  (color online)

In this paper the incident light wave is incident at the normal angle, but the tolerance of the incident light angle should be taken into account. When the incident light angle deviates from  $0^\circ$ , the diffraction efficiencies of the  $\pm 1\text{st}$  and  $\pm 2\text{nd}$  orders will no longer be equal. The diffraction efficiencies of the all four diffraction orders for the both polarizations vary with the angle of incidence deviation as shown in Fig. 4 for the optimum structure. However, the diffraction efficiency of the  $\pm 1\text{st}$  as well as the  $\pm 2\text{nd}$  orders are above 20% for both polarizations when the angle range

is  $-0.625^\circ$  to  $0.625^\circ$ .

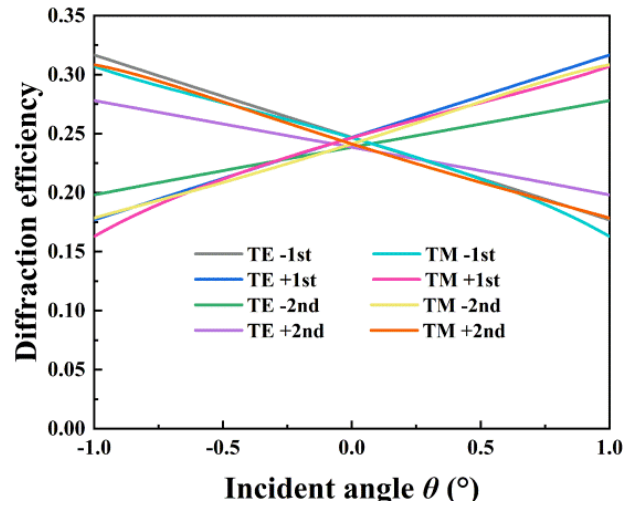


Fig. 4. The relationship between efficiency and incident angle for both two polarizations with  $\lambda=118.83 \mu\text{m}$ ,  $d=257.10 \mu\text{m}$ ,  $f=0.349$ , and  $h_1=213.20 \mu\text{m}$  (color online)

#### 3.2. Discussion of results and tolerance analysis

The thickness of the grating ridge has an effect on the propagation of the incident light in the grating region and can directly affect the phase difference of the coupled light waves. Fig. 5 shows the isogram of  $h_1$  and  $d$  with diffraction efficiency at normal incidence of incident light ( $\lambda=118.83 \mu\text{m}$ ), with the intersection of the white dashed lines ( $h_1=213.20 \mu\text{m}$ ,  $d=257.10 \mu\text{m}$ ) being the optimum value of  $h_1$  and  $d$  after optimization. As shown in Figs. 5 (a, b) for TE polarization, the diffraction efficiencies of  $\pm 1\text{st}$  and  $\pm 2\text{nd}$  orders are 24.72% and 23.82% for  $h_1=213.20 \mu\text{m}$  and  $d=257.10 \mu\text{m}$ , respectively. Furthermore, the total diffraction efficiency and uniformity are 97.08% and 1.85%, respectively. With the same range of considerations, Figs. 5 (c, d) show the diffraction efficiencies of  $\pm 1\text{st}$  and  $\pm 2\text{nd}$  orders under TM polarization, 24.64% and 24.12%, for a total diffraction efficiency and uniformity of 97.52% and 1.07%. Also, the diffraction efficiencies of all orders for both two polarizations are above 20% for  $h_1$  range of 212.70-213.70  $\mu\text{m}$  and  $d$  range of 256.64-257.40  $\mu\text{m}$ . In particular, the diffraction efficiency of 0 order is well constrained under TM and TE polarizations.

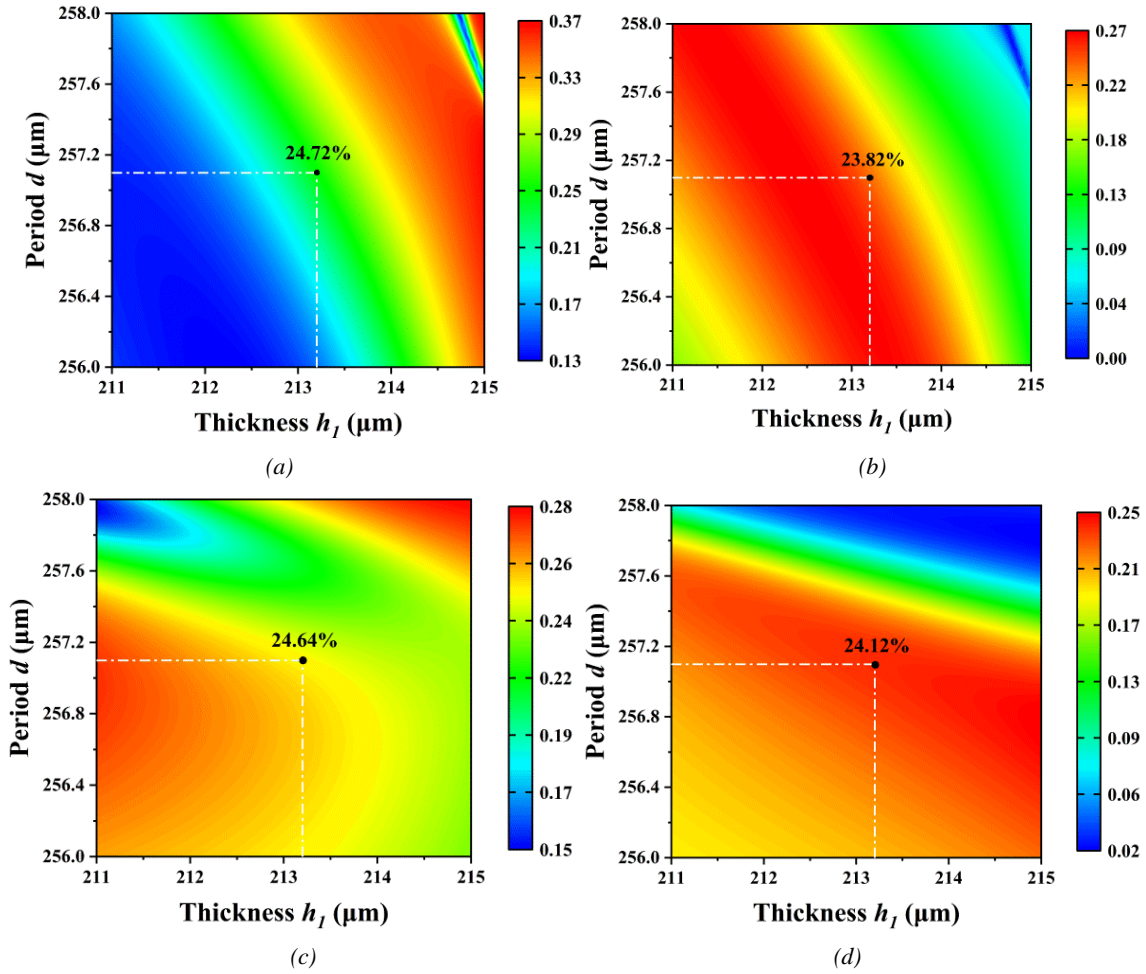


Fig. 5. The isogram of grating ridge thickness  $h_1$  and grating period  $d$  with diffraction efficiency under normal incidence with  $\lambda=118.83 \mu\text{m}$ , and  $f=0.349$ : (a) 1st order of TE polarization, (b) 2nd order of TE polarization, (c) 1th order of TM polarization, (d) 2nd order of TM polarization (color online)

In practice, the process of etching the grating will introduce certain structural deviations, so the manufacturing tolerance of the grating needs to be considered and duty cycle  $f$  as an important structural parameter of the grating should be taken into account. Fig. 6 shows the relationship between the grating duty cycle  $f$  and the diffraction efficiency. The diffraction efficiencies of all four diffraction orders under two polarizations exceed 21% at  $118.83 \mu\text{m}$  incident light at normal incidence while  $f$  range of  $0.348688-0.349264$ , with the best diffraction efficiency for each diffraction order at  $f=0.349$ . This shows that the target grating has good manufacturing tolerances and is well suited for practical applications.

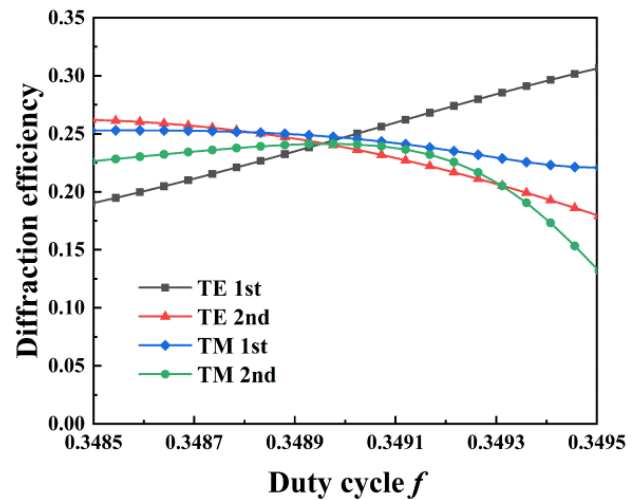


Fig. 6. Reflection efficiency at different duty cycle for both two polarizations under normal incidence with the parameters of  $\lambda=118.83 \mu\text{m}$ ,  $d=257.10 \mu\text{m}$ , and  $h_1=213.20 \mu\text{m}$  (color online)

Finally, the processing of this absorber is briefly described in the light of recent developments in processing technology. In the target structures of this paper, Al substrates can be prepared using methods such as chemical vapor deposition (CVD) and electron beam evaporation. In addition, the dielectric Si ridge arrays may be fabricated experimentally and can be obtained by electron beam lithography (EBL) and dry etching methods of preparation.

#### 4. Conclusion

In summary, a terahertz four-port polarization-independent reflective grating beam splitter has been proposed in this paper. By optimizing the grating parameters through RCWA and SA, the diffraction efficiencies of the  $\pm 1$ st and  $\pm 2$ nd orders of the target grating are 24.72% and 23.82% under TE polarization at 118.83  $\mu\text{m}$  wavelength normal incidence, respectively. Meanwhile the diffraction efficiencies of the  $\pm 1$ st and  $\pm 2$ nd orders under TM polarization are 24.64% and 24.12%, respectively, while the 0th order is better suppressed. The target grating also exhibits good polarization-independent properties. Further, the transmission mechanism inside the grating is analyzed by using FEM to make an electric field energy distribution map. In addition, a tolerance analysis is performed for different grating parameters, and the results show that the grating has good tolerances. In particular, the target grating beam splitter is simple in structure, easy to fabricate and scalable in function, and is of great application in its development.

#### Acknowledgements

This work is supported by the Science and Technology Program of Guangzhou (202002030284, 202007010001).

#### References

- [1] Y. Zhang, G. Xu, Z. Zheng, *Wave Random Complex* **31**(6), 2466 (2021).
- [2] G.-M. Lai, Y.-X. Wang, S. Liu, S.-Y. Zhong, *Wave Random Complex* **31**(3), 562 (2021).
- [3] S. Ding, Q. Li, Y. Li, Q. Wang, *Opt. Lett.* **36**(11), 1993 (2011).
- [4] J. Gou, T. Zhang, J. Wang, Y. Jiang, *Nanoscale Res. Lett.* **12**, **91** (2017).
- [5] M. Agour, C. Fallorf, F. Table, E. Castro-Camus, M. Koch, R. Bergmann, *Opt. Express*. **30**(5), 7068 (2022).
- [6] R. Arunkumar, J. K. Jayabarathan, S. Robinson, *J. Optoelectron. Adv. M.* **21**(7-8), 435 (2019).
- [7] Z. Guo, J. Xiao, *Opt. Commun.* **488**, 126850 (2021).
- [8] Z. Huang, B. Wang, Z. Lin, K. Wen, Z. Meng, Z. Nie, F. Zhang, X. Xing, L. Chen, L. Lei, J. Zhou, *J. Optoelectron. Adv. M.* **23**(9-10), 439 (2021).
- [9] J. F. G. Santos, C. H. S. Vieira, *Eur. Phys. J. Plus* **136**(3), 323 (2021).
- [10] Y. Zhang, B. Li, C. Xia, Z. Hou, G. Zhou, *Opt. Commun.* **475**, 126245 (2020).
- [11] P. Tian, W. Bi, X. Wang, W. Jin, B. Zhang, X. Fu, G. Fu, *Optik* **231**, 166461 (2021).
- [12] K. Zelaya, V. Hussin, O. Rosas-Ortiz, *Eur. Phys. J. Plus* **136**(5), 534 (2021).
- [13] Y. Zhan, F. Lin, Z. Song, Z. Sun, M. Yu, *Optik* **229**, 166122 (2021).
- [14] F. Chen, J. Zhang, J. Ma, C. Wei, R. Zhu, B. Han, Q. Wang, *Opt. Commun.* **444**, 45 (2019).
- [15] T. Xiaolin, W. Yong, Z. Qiang, L. Yunzhou, L. Huanxin, Q. Jiaojiao, Z. Dongbin, *Optik* **248**, 168054 (2021).
- [16] A. Zaltron, M. Merano, G. Mistura, C. Sada, F. Seno, *Eur. Phys. J. Plus* **135**(11), 896 (2020).
- [17] M. Abolhassani, *Optik* **231**, 166337 (2021).
- [18] E. Calloni, Archimedes Collaboration, Virgo Collaboration, *Eur. Phys. J. Plus* **136**(3), 335 (2021).
- [19] M. I. Marqués, S. Edelstein, P. A. Serena, *Eur. Phys. J. Plus* **136**(2), 185 (2021).
- [20] M. R. R. Vaziri, A. M. Beigzadeh, F. Ziaie, M. Yarahmadi, *Eur. Phys. J. Plus* **135**(5), 436 (2020).
- [21] N. Guo, Q. Zhao, H. Fan, H. Yu, X. Cui, M. Lv, T. Li, *Optik* **242**, 166269 (2021).
- [22] H. Li, B. Li, S. Wang, Z. Li, J. Qi, M. Yu, Y. Huang, Y. Li, A. Barbutis, J. Lubeck, R. Klein, S. Kroth, W. Paustian, M. Ressin, R. Thornagel, *Opt. Commun.* **475**, 126254 (2020).
- [23] Q. Zheng, J. Zhou, Q. Chen, L. Lei, K. Wen, Y. Hu, *IEEE Photon. J.* **11**(6), 2400410 (2019).
- [24] H. Li, K. Wang, L. Qian, *Optik* **207**, 164432 (2020).
- [25] X. Mu, Z. Chen, L. Cheng, S. Wu, A. Pepe, X. Tu, H. Y. Fu, *Opt. Commun.* **482**, 126562 (2021).
- [26] Z. Huang, B. Wang, *Laser Phys.* **31**, 126202 (2021).
- [27] H. Huang, S. Ruan, T. Yang, P. Xu, *Nano-Micro Lett.* **7**, 177 (2015).
- [28] Y. Zheng, X. Kai, P. Gao, J. Duan, *Optik* **201**, 163490 (2020).
- [29] M. G. Moharam, D. A. Pommet, E. B. Grann, T. K. Gaylord, *J. Opt. Soc. Am. A* **12**(5), 1077 (1995).
- [30] B. Gong, H. Wen, H. Li, *IEEE Photon. J.* **12**(2), 6500208 (2020).
- [31] W.-C. Liu, G. Jin, Y.-F. Xie, P. Sun, B. Zhou, W. Jia, J. Wang, C. Zhou, *Opt. Commun.* **488**, 126864 (2021).
- [32] X. Chai, Y.-P. Lu, X.-X. Chen, X. Wei, Q. Zhao, *Optik* **244**, 166623 (2021).
- [33] M. Ou, L. Liu, Y. Liu, L. Lan, S. Xie, X. Shi, *Optik* **225**, 165722 (2021).
- [34] B. Liu, C. Li, S. Zhang, J. He, *Optik* **209**, 164496 (2020).
- [35] M. A. Butt, S. N. Khonina, N. L. Kazanskiy, *Wave Random Complex* **31**(1), 146 (2021).

- [36] Y. Xu, F. Wang, Y. Gao, W. Chen, C. Chen, X. Wang, Y. Yi, X. Sun, D. Zhang, *Opt. Commun.* **463**, 125418 (2020).
- [37] Y. Kaya, A. Polat, T. Ş. Özşahin, *Eur. Phys. J. Plus* **135**(1), 89 (2020).

- [38] A. D. Rakić, A. B. Djurišić, J. M. Elazar, M. L. Majewski, *Appl. Opt.* **37**, 5271 (1998).

---

\*Corresponding author: wangb\_wsx@yeah.net